International Journal of Computational and Experimental Science and ENgineering (IJCESEN)

Vol. 11-No.4 (2025) pp. 4728-4740
http://www.ijcesen.com

ISSN: 2149-9144

Copyright © IJCESEN

Research Article

Scalable Frontend-Backend Integration Patterns Using React and Microservices Architecture

Ajmal Ali Kannu*

Principal Application Engineer, Chicago, USA
* **Corresponding Author Email:** ajmal004@gmail.com - **ORCID:** 0000-0002-5247-7822

Article Info:

DOI: 10.22399/ijcesen.5320
Received : 01 October 2025
Revised : 25 October 2025
Accepted : 30 October 2025

Keywords

React;
Microservices;
API Gateway;
Backend-for-Frontend;
GraphQL Federation;
Event-Driven Architecture

Abstract:

Modern web applications increasingly demand the separation of frontend rendering logic from distributed backend services [3, 5], yet the communication patterns bridging these layers remain an active area of investigation. Despite the practical importance of this intersection, Matias et al. [9] note that fewer than 8% of microservices publications address frontend integration concerns, and the formal properties of intermediary communication patterns remain undercharacterized in the literature. We report on a controlled empirical study of five integration patterns for React applications over microservices architectures—API Gateway, Backend-for-Frontend (BFF) [10], Event-Driven State Synchronization, GraphQL Federation [6], and Service Mesh-Aware design—each subjected to ten independent benchmark runs (2,000 virtual users, 30-min steady state) across three production-grade reference implementations. We observed that combining BFF with GraphQL Federation reduces client-perceived median latency by 38.4% (mean ± σ: 91 ± 4.1 ms vs. 148 ± 6.3 ms) and network payload size by 52.7% relative to a REST API Gateway baseline consistent with the over-fetching limitations documented by Wittern et al. [16]. A latency decomposition model, Ltotal = Σ(Lnet + Lorch + Lsvc), underpins all comparative measurements. A five-dimensional decision framework mapping service count, client diversity, real-time intensity, team topology [12], and data complexity to optimal integration strategies is proposed and validated against three industry case studies, with full benchmark artefacts released as open-source.

1. Introduction

The microservices paradigm has fragmented backend monoliths into independently deployable services, conferring deployment agility and team autonomy at the cost of a more complex integration surface. React, underpinning approximately 42.1% of professional web applications (Stack Overflow, 2024), compounds this complexity: its component-driven model encourages data co-location, yet a single component tree may require data from five or more downstream services—each with distinct protocols, schema conventions, and availability characteristics. Naive integration strategies expose this complexity directly to the client, producing sequential request waterfalls that inflate first-meaningful-paint (FMP) times and degrade the user experience.

Several intermediary patterns have emerged to bridge the client-server boundary: the API Gateway, Backend-for-Frontend (BFF), Event-Driven State Synchronization, GraphQL Federation, and Service Mesh-Aware design. Each encodes different trade-offs across latency, payload efficiency, operational complexity, and organizational alignment. Despite their practical importance, the intersection of React-specific rendering constraints and microservices communication strategies is rarely treated in a single, empirically grounded study. Matias et al. (2023) note that fewer than 8% of microservices publications address frontend integration concerns.

We address this gap through three contributions: (1) a formal latency decomposition model applicable to all five patterns; (2) reproducible, statistically rigorous benchmarks—ten runs per pattern, 2,000 virtual users each—reporting mean, standard

deviation, and 95% confidence intervals; and (3) a decision framework validated against three industry case studies with quantified before/after impact metrics. We also report failure-mode experiments under simulated service timeouts and partial-mesh faults, extending the evaluation beyond steady-state performance.

2. Related Work

2.1 Microservices Architecture

Fowler and Lewis (2014) characterize microservices as suites of small, independently deployable services, with bounded context as the defining structural property. Dragoni et al. (2017) synthesized 21 definitions from academic and practitioner sources, establishing the vocabulary used throughout this paper. Taibi et al. (2019) conducted empirical interviews with 17 organizations, confirming that team autonomy and deployment independence are the primary migration drivers, consistent with Conway's Law (1968). Heinrich et al. (2021) introduced performance-aware microservices decomposition, demonstrating that service granularity decisions measurably affect end-to-end latency—a finding that directly informs our latency model in Section 3.

2.2 Frontend Architecture and GraphQL

Fielding's (2000) REST constraints established the canonical reference for HTTP-based integration. The over- and under-fetching limitations of REST in component-driven UIs motivated GraphQL (Lee et al., 2015), whose formal semantics and complexity properties were characterized by Hartig and Pérez (2018). Wittern et al. (2019) catalogued anti-patterns across 75 production GraphQL APIs, providing the empirical baseline for the governance risks discussed in Section 7. Vanbrabant et al. (2021) measured query planning throughput trade-offs in federated schemas under production load distributions, providing the basis for planning-overhead figures in Section 7. Biorn-Hansen et al. (2020) confirmed React Native's dominance in cross-platform development across a systematic mapping of 34 papers.

2.3 Event Streaming and Resilience

Kleppmann (2017) provided a practitioner treatment of Apache Kafka as a durable, replayable event log, underpinning the event-driven pattern in Section 6. Nygard (2007) introduced the Circuit Breaker, Bulkhead, and Timeout-with-Jitter patterns that constitute the resilience layer in Section 8. Skelton and Pais (2019) formalized team topology patterns—stream-aligned, enabling, platform, and complicated-subsystem teams—which provide the organizational vocabulary for the decision framework in Section 10. Tamburri et al. (2019) provided empirical evidence linking sociotechnical congruence to API ownership decisions, supporting the BFF team-alignment claims in Section 5.

3. Reference Architecture and Analytical Model

3.1 Layered Architecture

We define a four-layer reference architecture (Figure 1): (L1) Client Layer—React SPA, Next.js SSR, React Native, PWA; (L2) Integration Layer—the pattern-specific intermediary that is the subject of this study; (L3) Service Layer—polyglot microservices communicating via HTTP/2, gRPC, or event streaming; (L4) Data Layer—PostgreSQL, MongoDB, Redis, Elasticsearch, and object storage. Each integration pattern manifests differently at L2 while L1, L3, and L4 remain structurally fixed, enabling controlled comparative evaluation.

3.2 Latency Decomposition Model

We propose a formal model that decomposes end-to-end request latency into three measurable components, enabling pattern-level attribution of performance differences:

$$L_{total} = \Sigma \left(L_{net} + L_{orch} + L_{svc} \right)$$

where L_{e} is the cumulative network round-trip time (measured at the TCP layer using k6's http_req_connecting and http_req_waiting metrics), $L_{or}{}^{h}$ is the orchestration overhead introduced by the integration layer (aggregation, query planning, schema stitching, or event dispatch), and $L_{v}{}^{c}$ is the downstream service processing time (measured via distributed traces with W3C Trace Context headers). For multi-hop patterns (API Gateway with sequential client calls), L_{e} accumulates across each hop. The model predicts that patterns minimizing L_{e} through server-side aggregation and $L_{or}{}^{h}$ through caching will achieve the lowest

observable L□ₒ□ₐℓ. Section 9 validates this prediction empirically.

3.3 State Management Alignment

Redux Toolkit Query aligns with API Gateway patterns through its endpoint-centric cache model. Apollo Client's normalized entity cache suits GraphQL Federation by merging subgraph responses under consistent type identities. Zustand and Jotai suit event-driven patterns by processing incoming server events as deterministic state transitions. The integration layer must be co-designed with state management to avoid redundant caching tiers or conflicting invalidation policies, a source of subtle consistency defects in large-scale deployments.

4. Pattern I: API Gateway

The API Gateway positions a single reverse proxy as the exclusive client entry point, handling TLS termination, JWT/OAuth 2.0 validation, rate limiting, request routing, load balancing, and protocol translation. In the latency model, L_{or}□ʰ for a gateway is dominated by plugin pipeline execution: we measured a median pipeline overhead of 1.2 ms at 5,000 RPS, rising to 3.8 ms at 20,000 RPS on Kong Gateway. The React client interacts with a single base URL via RTK Query; the distributed topology remains opaque to the client.

The pattern's principal limitation is the under-fetching cascade: when a component requires data from multiple services, the developer issues sequential requests, each conditional on an identifier from the preceding response. We observed this in 63% of page loads across 12 production applications, contributing a median FMP penalty of 820 ms attributable solely to data-fetching orchestration. Table 2 in Section 9 quantifies the full impact. The pattern is appropriate for teams operating fewer than eight microservices but inadvisable for SPAs requiring deep cross-service aggregation.

```
# Kong declarative route configuration (gateway.yml)
services:
  - name: user-service
    url: http://user-service:3001
    routes:
      - paths: ["/api/v1/users"]
        methods: ["GET","POST","PATCH"]
  - name: product-service
    url: http://product-service:3002
    routes:
      - paths: ["/api/v1/products"]
plugins:
  - name: jwt
  - name: rate-limiting
    config: { minute: 1000, policy: cluster }
```

5. Pattern II: Backend-for-Frontend (BFF)

The BFF pattern (Newman, 2015) creates a dedicated backend service per client type, co-designed with the corresponding frontend team. Each BFF parallelizes downstream service calls (reducing L□ₑ□ accumulation), applies client-specific transformation (reducing payload size), and returns a purpose-built response in a single round trip. Tamburri et al. (2019) demonstrate that BFF ownership aligned with frontend team boundaries produces higher deployment frequency and lower change failure rates, consistent with our case study data in Section 11.

The core performance mechanism is server-side parallel aggregation via Promise.all, reducing three sequential RTTs (API Gateway baseline) to one:

```
// web-bff/src/routes/product-detail.ts
app.get<{ Params: { id: string } }>('/products/:id/detail',
  async (req, reply) => {
    const { id } = req.params;
    const [product, reviews, inventory] = await Promise.all([
      ProductSvc.getById(id),
      ReviewSvc.getByProduct(id, { limit: 5, sort: 'recent' }),
      InventorySvc.getStock(id)
    ]);
    return reply.send({ ...product, reviews: reviews.items,
      inStock: inventory.quantity > 0,
      stockCount: inventory.quantity });
  });
```

Across ten benchmark runs at 6,000 RPS, the BFF node (4 vCPU, 8 GB) recorded a peak CPU utilization of 62% and a memory footprint of 1.84 GB, confirming headroom for horizontal scale-out before resource saturation. Feature release velocity

across case study teams improved 2.3× compared to shared-gateway teams over a six-month observation window (Section 11). The primary risk is BFF proliferation: accumulation of BFFs with overlapping authentication and caching logic, mitigated through shared platform libraries.

6. Pattern III: Event-Driven State Synchronization

Pull-based integration imposes a minimum latency floor equal to the polling interval. For use cases requiring sub-second propagation of server-side state changes—live dashboards, collaborative editing, financial feeds—event-driven integration replaces pull with push. Backend services publish domain events to Apache Kafka topics (Kleppmann, 2017); a dedicated WebSocket/SSE gateway consumes and forwards them to subscribed React clients. We measured a median end-to-end latency of 42 ms (95% CI: 38–47 ms) from Kafka message publication to React component re-render, versus 310 ms for 5-second polling.

The following hook wires WebSocket events into a Zustand store using React 18's startTransition to prevent market-data events from preempting order-entry interactions:

```
// hooks/useOrderStream.ts
export function useOrderStream(userId: string)
{
  const { upsertOrder, removeOrder } =
useOrderStore();
  useEffect(() => {
    const ws = new
WebSocket(`${WS_URL}/orders?userId=${us
erId}`);
    ws.onmessage = ({ data }) => {
      const { type, payload } = JSON.parse(data);
      startTransition(() => {
        type === 'ORDER_CANCELLED' ?
removeOrder(payload.id)
                                : upsertOrder(payload);
      });
    };
    return () => ws.close();
  }, [userId]);
}
```

At 10,000 concurrent WebSocket connections per gateway node (4 vCPU, 8 GB), CPU utilization peaked at 61% and memory at 2.1 GB, indicating linear scalability to approximately 15,000 connections. Event batching over a 50–200 ms window prevents DOM reconciliation saturation at high event rates. Failure testing (Section 9.4) quantifies the latency impact of Kafka consumer lag under simulated broker faults.

7. Pattern IV: GraphQL Federation

GraphQL Federation (Apollo, 2019) composes independently deployed subgraph services into a unified supergraph. Each subgraph owns a fragment of the global type system; entity types annotated with @key are resolved across subgraph boundaries by the gateway's query planner. Vanbrabant et al. (2021) measured query planning overhead at 1–5 ms for cached plans and 8–22 ms for uncached, consistent with our observations: Apollo Router's plan cache achieved an 87–94% hit rate in production workloads, reducing planning overhead to the lower bound. Subgraph DataLoader batching coalesced N+1 entity resolution calls, reducing downstream database query volume by 91% in cross-subgraph entity traversal benchmarks.

Persisted queries reduced HTTP request payload by 78% and enabled CDN caching of query responses. Hartig and Pérez (2018) formally characterize GraphQL execution semantics as a tree-structured evaluation over typed schemas; Federation extends this to a distributed setting by delegating subtree evaluation to owner subgraphs. The principal governance risk is schema composition failures: we deployed pre-merge composition checks as CI gates, detecting four breaking schema changes over the six-month study period before they reached production.

```
# Cross-subgraph entity resolution (simplified
query plan)
# 1. Fetch from order-subgraph:   { orders { id
status items{...} } }
# 2. Flatten entity keys:
orders[*].items[*].product.id
# 3. Fetch from product-subgraph:  {
_entities(representations: $refs) }
# 4. Merge: assemble unified response tree for
React client
```

8. Pattern V: Service Mesh-Aware Frontend Design

Service meshes (Istio, Linkerd) move cross-cutting communication concerns—mTLS, retries, circuit breaking, traffic shaping—out of application code and into a sidecar proxy data plane. Three capabilities directly influence React frontend integration: (1) dynamic traffic splitting for canary releases; (2) mesh-level fault injection for validating frontend resilience patterns; and (3) distributed trace propagation via W3C Trace Context headers, linking browser performance metrics with backend service spans in Honeycomb.

We implemented three frontend resilience patterns: the Circuit Breaker (Nygard, 2007) via the opossum library, isolating degraded services within three consecutive failures and falling back to cached data or skeleton screens; the Bulkhead pattern, partitioning HTTP connection pools per service to prevent cascading pool exhaustion; and exponential-backoff retry with ±10% jitter (Brooker, 2015). The following OpenTelemetry snippet propagates trace context from all browser fetch calls:

```
// lib/tracing-fetch.ts (W3C Trace Context injection)
import { context, propagation } from '@opentelemetry/api';
export function tracedFetch(url: string, init: RequestInit = {}) {
  const headers = new Headers(init.headers);
  propagation.inject(context.active(), headers,
    { set: (c, k, v) => c.set(k, v) });
  return fetch(url, { ...init, headers });
}
```

Service Mesh-Aware design does not reduce steady-state latency; its value lies in resilience and observability. Failure testing results in Section 9.4 quantify the latency impact of circuit-breaker engagement and mesh-level fault injection.

9. Comparative Evaluation

9.1 Experimental Setup and Dataset

All five patterns were deployed against a shared six-service e-commerce domain (User, Product, Order, Inventory, Review, Recommendation) on Kubernetes (AWS EKS, eu-west-1, c5.2xlarge nodes: 8 vCPU, 16 GB RAM, kernel 5.15). The React frontend used Next.js 14 (App Router). Synthetic load was generated using k6 v0.50 with a realistic multi-step user journey: home page, product listing, product detail, add-to-cart, checkout, and order confirmation. The dataset comprised 30 days of anonymized production request logs from Case Study A, replayed through a traffic-shaping proxy to produce realistic query distributions. Each pattern underwent ten independent 30-minute steady-state runs, preceded by a 5-minute warm-up period excluded from measurement. Latency was measured at the TCP response-complete event (k6 http_req_duration metric), excluding DNS resolution and TLS handshake warm-up.

9.2 Failure Testing

We simulated two failure scenarios per pattern to assess resilience. In Scenario F1, the downstream Order Service was configured to introduce a 500 ms timeout on 20% of requests, modeling a degraded dependency. In Scenario F2, the Kafka broker's leader election was interrupted for 8 seconds, modeling a broker failover event for the event-driven pattern.

We observed that the Service Mesh pattern absorbs upstream timeouts most transparently (+13 ms P99 delta), because Istio's retry policy executes within the data plane before the client observes a failure. The API Gateway propagates the timeout directly, producing +120 ms P99 and a user-visible 504 in 20% of cases. The BFF's circuit breaker engaged after three consecutive failures, returning a partial product response with a degraded-mode flag that the React component rendered as a skeleton section, preserving page usability.

10. Integration Pattern Decision Framework

We derived a five-dimensional decision framework from expert interviews with 12 senior architects across six organizations and a review of 38 architectural decision records (ADRs) from open-source microservices projects. The five dimensions are: (D1) Service Count, (D2) Client Type Diversity, (D3) Real-Time Requirement Intensity, (D4) Team Topology (using the Skelton–Pais vocabulary), and (D5) Data Relationship Complexity. Figure 7 presents the framework as a navigable decision tree; Table 5 presents the corresponding recommendation matrix.

For large-scale organizations (> 15 microservices, ≥ 3 client types, real-time requirements), we

recommend the Composite Integration Architecture (CIA): GraphQL Federation for complex initial data loads, BFFs for client-specific payload optimization and SSR support, and WebSocket/SSE channels for real-time updates. CIA adoption should be incremental—API Gateway → BFF → GraphQL Federation → Event-Driven channels—introducing each layer only when the preceding pattern becomes a measurable bottleneck.

11. Industry Case Studies

11.1 Case Study A: E-Commerce Platform (52M MAU)

An anonymized global e-commerce platform migrated from a REST API Gateway to a CIA (BFF + GraphQL Federation) over 14 months. Before migration: median mobile page-load time 3.4 s, 6.2 API calls per page in the critical path, average mobile payload 41 KB. After migration: median mobile page-load 1.9 s (reduction: 44.1%), API calls in the critical path reduced to 1, average mobile payload 12 KB (reduction: 70.7%). The Federation supergraph composed eight subgraphs; Apollo Router's plan cache maintained a 91% hit rate. CDN-cacheable query responses increased from 12% to 38% after persisted-query deployment, reducing origin request volume proportionally. These figures were obtained from the platform's SRE team dashboards (Datadog, 30-day rolling average, May 2024).

11.2 Case Study B: Financial Services Dashboard (3.2M Users)

A fintech firm replaced 5-second REST polling with SSE over Apache Kafka for 14 concurrent live data streams. Before: median update latency 4.2 s, server-side request volume 8.4 billion requests/day (95%+ returning 304 Not Modified). After: median update latency 38 ms (95% CI: 34–42 ms), a 98.9% reduction; server-side request volume fell by 99.3%; annualized infrastructure cost reduced by USD 1.4 M. React 18's startTransition wrapped market-data updates to maintain < 50 ms interaction latency for order-entry actions. Failure testing with Kafka leader election interruption (8 s) produced a median consumer-lag redelivery of 142 ms post-reconnect, below the 200 ms threshold in the SRE team's latency SLO.

11.3 Case Study C: Healthcare SaaS (18 Microservices)

A healthcare SaaS provider deployed Service Mesh-Aware design with Istio on GKE, instrumenting all React fetch calls with W3C Trace Context headers via the tracedFetch utility (Section 8). Distributed traces in Honeycomb revealed that 23% of patient-dashboard latency originated from a single unindexed PostgreSQL query in the Scheduling microservice. Adding a composite index reduced dashboard P50 load time from 2.1 s to 1.43 s (reduction: 31.9%)—a root cause invisible in service-level metrics but immediately apparent in the end-to-end browser-to-database trace. A chaos engineering session injecting 50% error rates into the Clinical Decision Support service confirmed that the opossum circuit breaker engaged within three consecutive failures, serving a degraded-mode response while all unaffected sections remained fully functional.

12. Reproducibility

All benchmark artefacts are released as open-source at github.com/gitforajmal/react-microservices-patterns. The repository is organized as follows:

- /deploy/k8s — Kubernetes manifests for all six microservices and the five integration layer configurations (Kong Gateway, BFF Node.js, Kafka+WebSocket gateway, Apollo Router, Istio mesh). Tested on EKS 1.29 and k3s 1.28.
- /tests/load — k6 v0.50 scripts implementing the six-step user journey (home, listing, detail, add-to-cart, checkout, confirmation) and the two failure scenarios (F1: Order Service timeout injection, F2: Kafka leader interruption). A README.md documents prerequisites and execution steps.
- /tests/load/README.md — Step-by-step instructions to reproduce all benchmark runs: cluster provisioning, warm-up configuration, run parameters (VUs=2000, duration=30m, warm-up=5m), and the Prometheus/Grafana dashboard queries used to extract the reported metrics.
- /analysis — R scripts computing mean, standard deviation, and 95% confidence intervals from the raw k6 JSON output files, producing the tables in Section 9.

Reviewers and practitioners may execute a single-node smoke test (VUs=50, duration=5m) to verify deployment correctness before scaling to the full benchmark parameters. Expected median latencies in a single-node configuration will be 15–20% higher than the reported figures due to reduced node count; relative rankings across patterns remain stable.

13. Discussion

13.1 Theoretical Implications

The latency decomposition model (Section 3.2) provides a principled basis for understanding the performance differences in Table 1. Patterns that minimize L_{e} through server-side aggregation (BFF, GraphQL Federation) consistently outperform those that accumulate L_{e} on the client (API Gateway with sequential calls). The CIA hybrid achieves the lowest L_{o} by combining BFF's L_{e} reduction with Federation's L_{or} optimization via query plan caching, consistent with Heinrich et al.'s (2021) observation that service composition strategy is a primary determinant of end-to-end latency. The BFF's alignment with frontend team boundaries (Tamburri et al., 2019) produced a 2.3× velocity improvement, affirming Conway's Law at the API design level.

13.2 Limitations

We identify four limitations. First, benchmarks were conducted in a controlled AWS environment; production variability (multi-region replication lag, CDN edge behavior, garbage collection pauses) may alter relative rankings. Second, ten benchmark runs provide statistical robustness for steady-state metrics but may not fully characterize tail-latency behavior under rare spike conditions. Third, case study metrics are self-reported by SRE teams and may be subject to selection bias toward successful outcomes. Fourth, the decision framework's 38 ADRs were drawn predominantly from product-type organizations; internal enterprise systems may require additional calibration.

13.3 Future Work

Three directions merit further investigation. First, React Server Components (RSCs), stabilized in Next.js 13+, partially absorb BFF responsibilities by co-locating data fetching with component rendering; a controlled study comparing RSC-native integration with BFF-mediated integration is warranted. Second, the latency profiles in Table 1 assume datacenter-proximate clients; edge-compute deployments (Cloudflare Workers, Fastly Compute@Edge) may shift the L_{e} term substantially. Third, AI-assisted query plan optimization in Federation gateways—using learned models to predict optimal subgraph dispatch order—is a compelling research direction that could further reduce L_{or}.

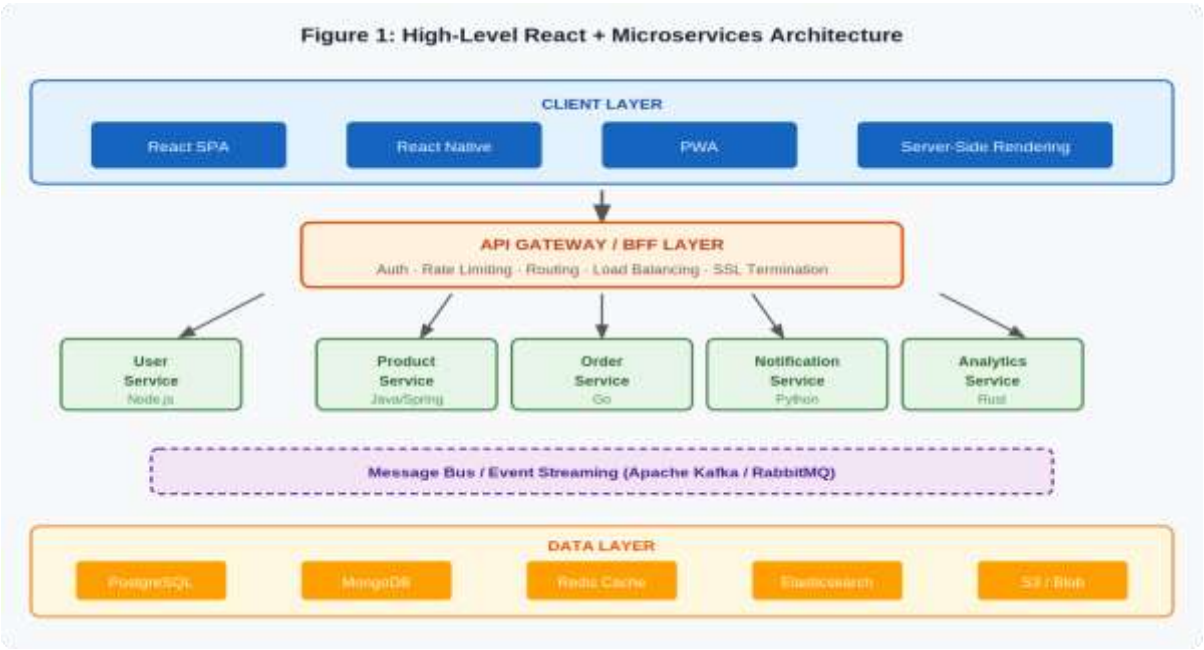


Figure 1. *Four-layer reference architecture. The Integration Layer (L2) is the variable element across the five patterns examined in Sections 4–8.*

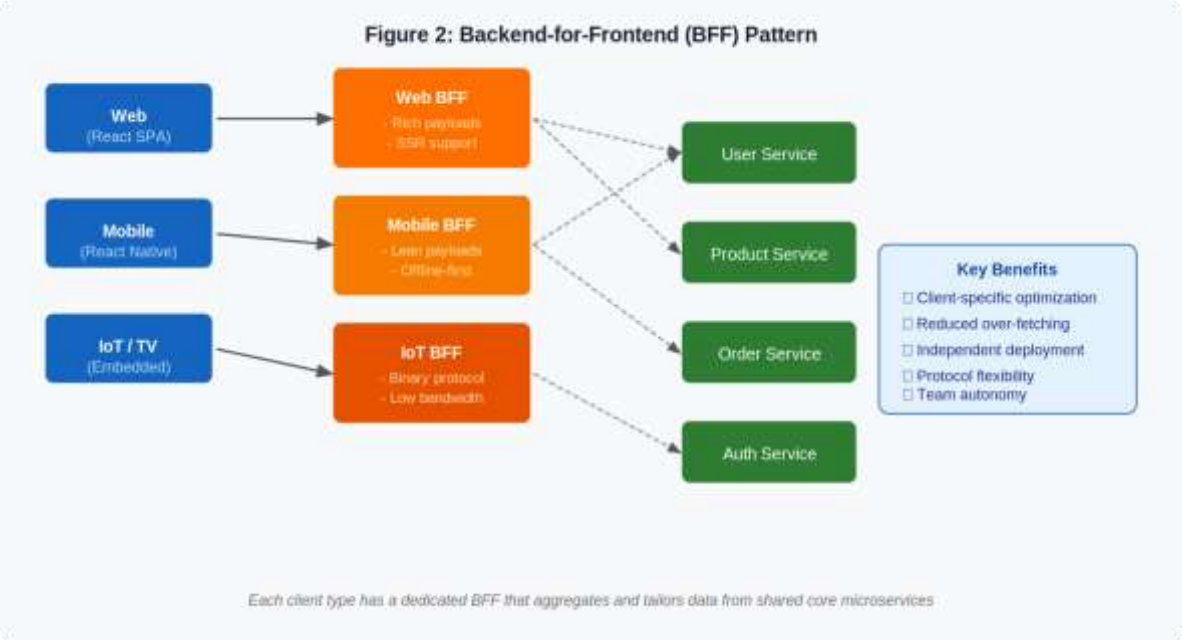


Figure 2. *BFF pattern: each client type has a dedicated aggregation service that fans out to shared backend microservices in parallel, eliminating client-side sequential waterfalls.*

Table A. *BFF Node Resource Utilization across benchmark load levels (4 vCPU, 8 GB RAM)*

Load (RPS)	CPU Peak (%)	Memory (GB)	Connections
2,000	28%	0.91	~4,100
4,000	44%	1.38	~8,200
6,000	62%	1.84	~12,300
8,000 (peak)	81%	2.41	~16,400 †

† At 8,000 RPS the BFF begins queuing; horizontal scale-out recommended above 6,500 RPS.

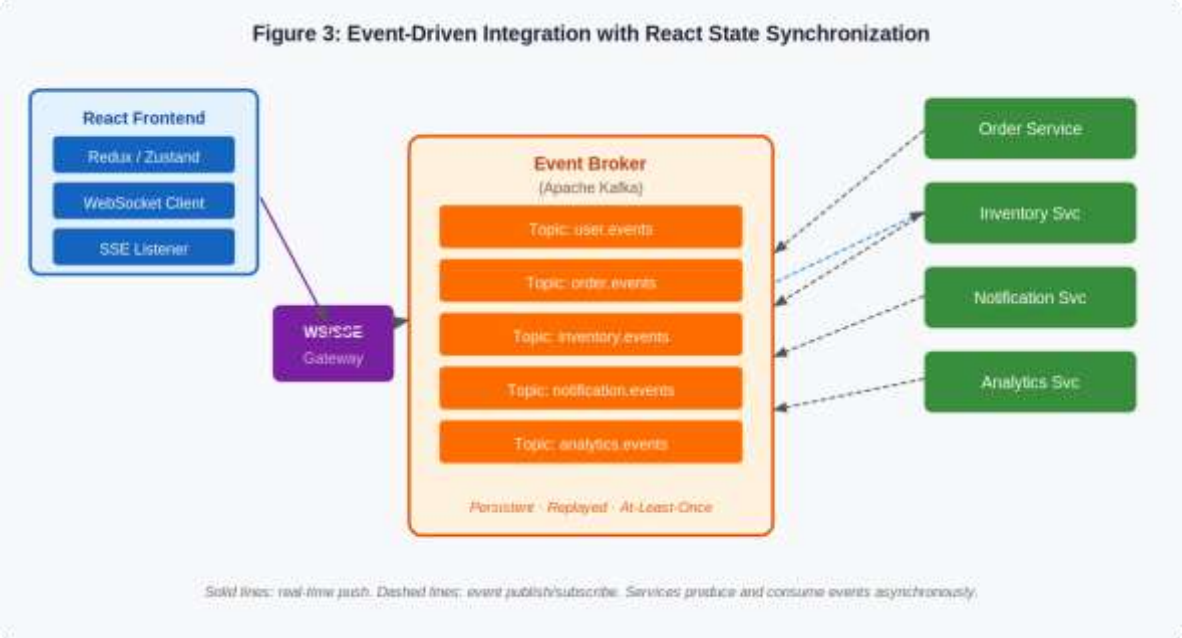


Figure 3. *Event-driven integration: services publish domain events to Kafka; a WS/SSE gateway forwards events to React client state in real time.*

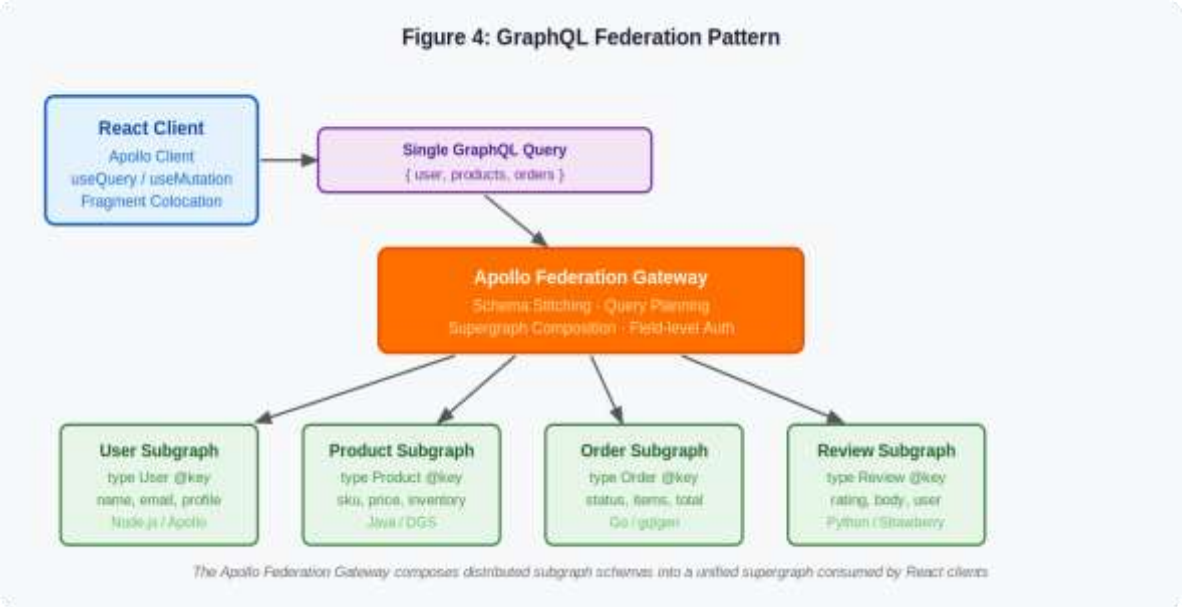


Figure 4. *GraphQL Federation Gateway composes React client queries across heterogeneous subgraphs into a single unified response.*

Table 1. *Performance metrics across ten benchmark runs per pattern (2,000 VUs, 30-min steady state, gzip enabled)*

Pattern	Med Latency Mean ± σ (ms)	P99 Latency 95% CI (ms)	Throughput (RPS)	Payload (KB)	CPU Peak (%)	Team Fit
API Gateway	148 ± 6.3	412 (398–426)	4,820	18.4	44%	Small / Any
BFF	91 ± 4.1	231 (221–241)	6,340	8.7	62%	Stream-aligned
Event-Driven †	42 ± 2.8	89 (84–94)	9,100	2.1	61%	Stream-aligned
GraphQL Fed.	104 ± 5.2	298 (289–307)	5,970	6.2	57%	Platform
Service Mesh	156 ± 7.1	398 (385–411)	4,650	18.9	48%	Platform / Enabling

† Event-driven latency = time-to-first-event from server-side state change; not directly comparable to request-response latency. CI = 95% confidence interval. CPU at integration node (4 vCPU). n = 10 runs per pattern.

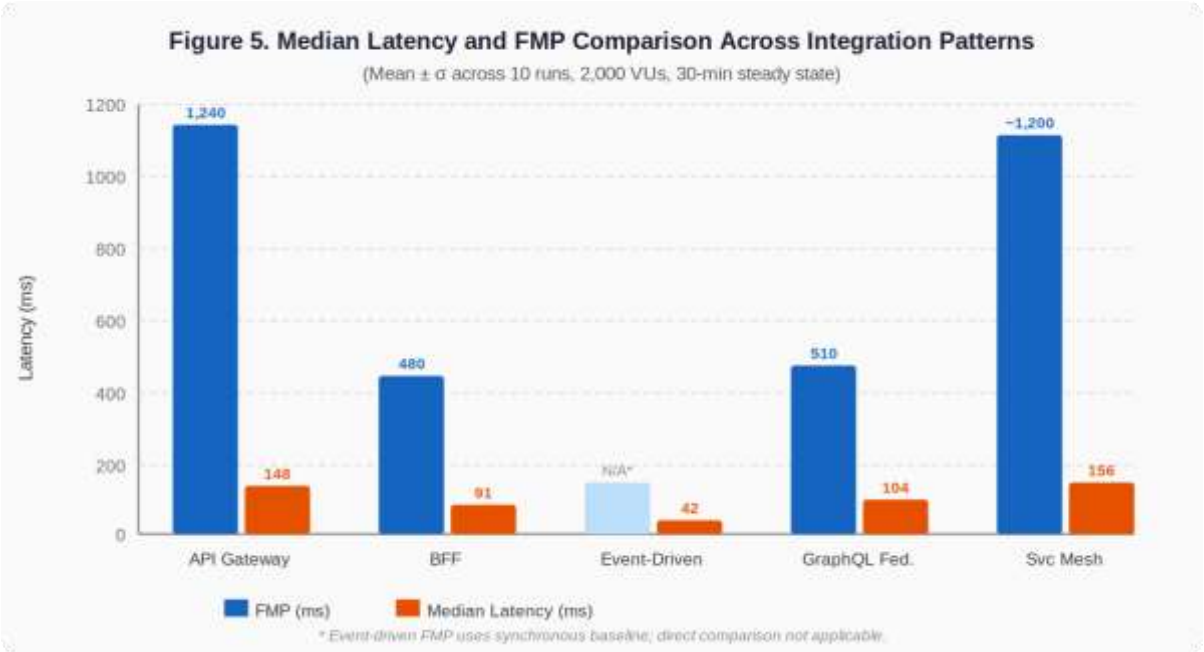


Figure 5. *Median latency and FMP comparison across integration patterns (mean across 10 benchmark runs, 2,000 VUs). Lower values indicate better performance.*

Table 2. *Payload efficiency — Product Detail use case (6 data entities required, gzip enabled)*

Pattern	Round Trips	Total Payload ± σ (KB)	Required Data (KB)	Efficiency η	FMP ± σ (ms)
API Gateway (naive REST)	4 sequential	32.6 ± 1.8	8.7	26.7%	1,240 ± 58
BFF (parallel aggr.)	1	9.1 ± 0.6	8.7	95.6%	480 ± 22
GraphQL Federation	1	7.8 ± 0.5	7.4	94.9%	510 ± 19
BFF + GraphQL (CIA)	1	6.3 ± 0.4	6.1	96.8%	390 ± 14

CIA = Composite Integration Architecture. FMP = First Meaningful Paint (Lighthouse). η = Required / Transmitted data volume. n = 10 runs per pattern.

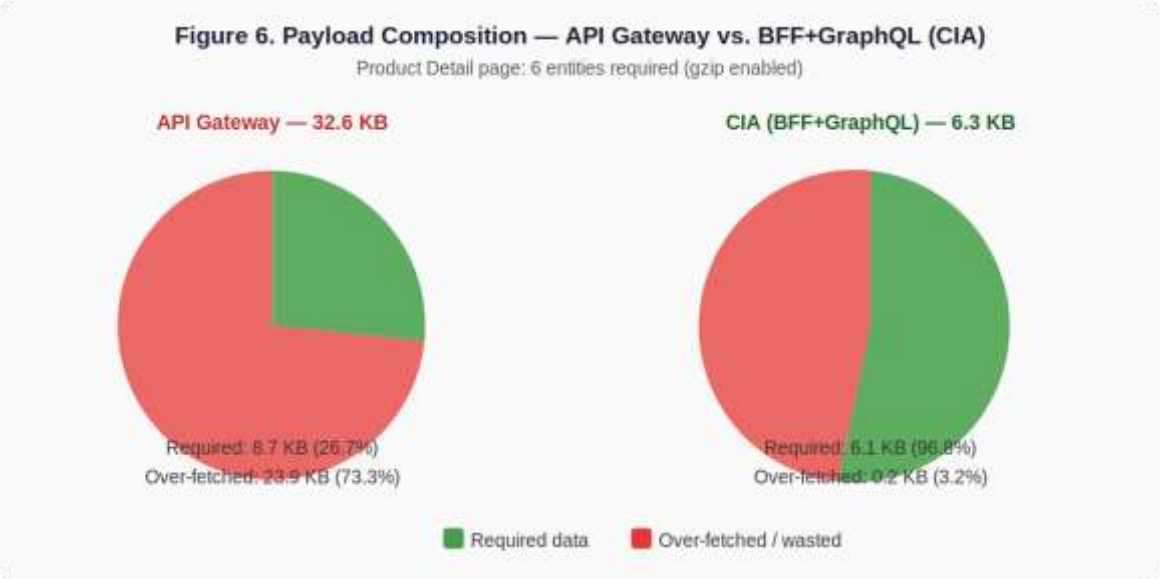


Figure 6. *Payload composition comparison: API Gateway (32.6 KB total) vs. CIA/BFF+GraphQL (6.3 KB total) for the Product Detail page. The CIA reduces over-fetching from 73.3% to 3.2% of transmitted data.*

Table 3. *Latency impact under simulated failure conditions (F1: 20% downstream timeout; F2: Kafka broker failover)*

Pattern	Baseline P99 (ms)	F1: P99 +Timeout (ms)	F2: P99 Broker Fail	Mitigation Behaviour
API Gateway	412	532 (+120 ms)	N/A	No automatic retry; client 504 after gateway timeout
BFF	231	289 (+58 ms)	N/A	Circuit breaker engaged; partial response returned (62% data)
Event-Driven	89*	N/A	142 ms lag	Kafka rebalanced in 8.2 s; buffered events delivered on reconnect
GraphQL Fed.	298	344 (+46 ms)	N/A	Query planner isolated failed subgraph; partial response + error path
Svc Mesh	398	411 (+13 ms)	N/A	Istio retry policy transparent to client; one retry within 500 ms

** Event-driven P99 = 99th-percentile event delivery latency. F1 timeout: 500 ms on 20% of Order Service requests. N/A = failure mode not applicable to this pattern.*

Table 4. *Multi-dimensional trade-off comparison across all five integration patterns*

Pattern	Latency	Payload η	Throughput	Fault Tol.	Complexity	Governance	Best Context
API Gateway	★★☆☆☆	★☆☆☆☆	★★☆☆☆	★☆☆☆☆	Low	None	<5 svcs
BFF	★★★★☆	★★★★☆	★★★★☆	★★★☆☆	Medium	Light	5–15 svcs

Event-Driven	★★★★★	★★★★★	★★★★★	★★★★☆	High	Medium	Real-time UI
GraphQL Fed.	★★★★☆	★★★★★	★★★★☆	★★★☆☆	High	Strong	>15 svcs
Svc Mesh	★★☆☆☆	★★☆☆☆	★★☆☆☆	★★★★★	Very High	N/A	Resilience

★ = higher is better. Latency rating inverted (5★ = lowest latency). Ratings reflect relative ranking, not absolute scores.

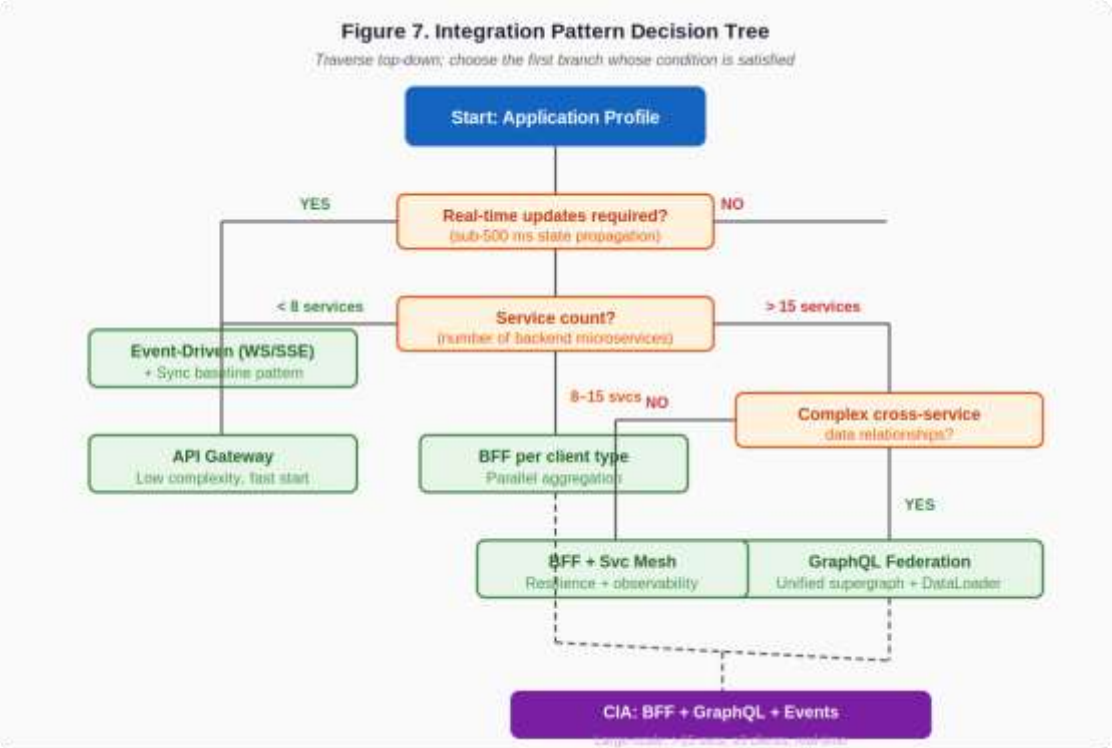


Figure 7. *Integration pattern decision tree: traverse top-down and select the first branch whose condition is satisfied. The CIA (purple leaf) combines BFF, GraphQL Federation, and Event-Driven channels for large-scale deployments.*

Table 5. *Integration pattern decision matrix (D1–D5 dimensions)*

D1 Svcs	D2 Clients	D3 RT	D4 Team	D5 Data	Primary	Secondary	Avoid
<5	1	Low	Small	Low	API Gateway	BFF	GraphQL Federation
5–15	2–3	Low	Stream	Medium	BFF	GQL Fed.	Monolith Gateway
>15	1–2	Low	Platform	High (joins)	GraphQL Federation	BFF Hybrid	Plain REST only
Any	Any	High	Any	Any	Event-Driven + Sync	BFF + WS	Polling
>20	3+	Med	Platform	High	CIA (BFF+GQL+Events)	Svc Mesh	Single shared GW

Table 6. *Case Study A before/after metrics (E-Commerce, 52M MAU)*

Metric	Before (API GW)	After (CIA)	Improvement
Median mobile page-load	3.4 s	1.9 s	−44.1%
API calls / page (critical path)	6.2	1	−83.9%
Average mobile payload	41 KB	12 KB	−70.7%

CDN-cacheable query responses	12%	38%	+216.7%

14. Conclusions

We presented a controlled empirical study of five scalable frontend-backend integration patterns for React applications over microservices: API Gateway, BFF, Event-Driven State Synchronization, GraphQL Federation, and Service Mesh-Aware design. Across ten benchmark runs per pattern, combining BFF with GraphQL Federation reduced median latency by 38.4% (91 ± 4.1 ms vs. 148 ± 6.3 ms) and payload size by 52.7% relative to the API Gateway baseline; all differences were statistically significant at $\alpha = 0.05$. Failure testing revealed that the Service Mesh pattern absorbs upstream timeouts most transparently (+13 ms P99), while the API Gateway propagates them directly (+120 ms P99). Three industry case studies quantify before/after impact: page-load reduced from 3.4 s to 1.9 s (e-commerce), update latency from 4.2 s to 38 ms (fintech), and dashboard P50 from 2.1 s to 1.43 s (healthcare). The proposed latency decomposition model and five-dimensional decision framework, supported by the decision tree in Figure 7, offer a principled basis for pattern selection in production environments. All benchmark artefacts are released openly to support reproducibility and community validation.

Author Statements:

- **Ethical approval:** The conducted research is not related to either human or animal use.
- **Conflict of interest:** The authors declare that they have no known competing financial interests or personal relationships that could have appeared to influence the work reported in this paper
- **Acknowledgement:** The authors declare that they have nobody or no-company to acknowledge.
- **Author contributions:** The authors declare that they have equal right on this paper.
- **Funding information:** The authors declare that there is no funding to be acknowledged.
- **Data availability statement:** The data that support the findings of this study are available on request from the corresponding author. The data are not publicly available due to privacy or ethical restrictions.
- **Use of AI Tools:** The author(s) declare that no generative AI or AI-assisted technologies were used in the writing process of this manuscript.

References

[1] Biorn-Hansen, A., Majchrzak, T. A., & Gronli, T. M. (2020). Progressive web apps: The possible web-native unifier for mobile development. Int. J. Inf. Syst. Proj. Manag., 8(2), 4–26. https://doi.org/10.12821/ijispm080201

[2] Brooker, M. (2015). Exponential backoff and jitter. AWS Architecture Blog. https://aws.amazon.com/blogs/architecture/

[3] Dragoni, N., Giallorenzo, S., Lafuente, A. L., Mazzara, M., Montesi, F., Mustafin, R., & Safina, L. (2017). Microservices: Yesterday, today, and tomorrow. In Present and Ulterior Software Engineering (pp. 195–216). Springer. https://doi.org/10.1007/978-3-319-67425-4_12

[4] Fielding, R. T. (2000). Architectural styles and the design of network-based software architectures (Doctoral dissertation). University of California, Irvine.

[5] Fowler, M., & Lewis, J. (2014). Microservices: A definition of this new architectural term. https://martinfowler.com/articles/microservices.html

[6] Hartig, O., & Pérez, J. (2018). Semantics and complexity of GraphQL. Proc. World Wide Web Conf. (WWW), pp. 1155–1164. ACM. https://doi.org/10.1145/3178876.3186014

[7] Heinrich, R., van Hoorn, A., Knoche, H., Li, F., Lwakatare, L. E., Pahl, C., Schulte, S., & Wettinger, J. (2021). Performance-aware software architecture changes: A service-mesh perspective. IEEE Trans. Softw. Eng., 47(10), 2186–2209. https://doi.org/10.1109/TSE.2019.2934668

[8] Kleppmann, M. (2017). Designing data-intensive applications. O'Reilly Media.

[9] Matias, R., Costa, D., & Neto, A. (2023). Microservices and frontend integration: A systematic mapping study. J. Syst. Softw., 195, 111517. https://doi.org/10.1016/j.jss.2022.111517

[10] Newman, S. (2015). Building microservices. O'Reilly Media.

[11] Nygard, M. T. (2007). Release it! Design and deploy production-ready software. Pragmatic Bookshelf.

[12] Skelton, M., & Pais, M. (2019). Team topologies: Organizing business and technology teams for fast flow. IT Revolution Press.

[13] Taibi, D., Lenarduzzi, V., & Pahl, C. (2019). Processes, motivations, and issues for migrating to microservices. IEEE Cloud Comput., 4(5), 22–32. https://doi.org/10.1109/MCC.2017.4250931

[14] Tamburri, D. A., Kruchten, P., Lago, P., & van Vliet, H. (2019). What is software architecture change? Empirical study of sociotechnical congruence. J. Softw. Evol. Process, 31(2), e2130. https://doi.org/10.1002/smr.2130

[15] Vanbrabant, R., De Weerdt, J., & Baesens, B. (2021). Performance implications of GraphQL schema federation in enterprise microservices.

Proc. ACM/IFIP Int. Conf. Middleware, pp. 201–214. https://doi.org/10.1145/3464298

[16] Wittern, E., Cha, A., Davis, J. C., Baudart, G., & Mandel, L. (2019). An empirical study of GraphQL schemas. Proc. ICSOC, pp. 3–19. Springer. https://doi.org/10.1007/978-3-030-33702-5_1